

# ClickTrain: Efficient and Accurate End-to-End Deep Learning Training via Fine-Grained Architecture-Preserving Pruning

Chengming Zhang

Washington State University  
Pullman, WA, USA  
chengming.zhang@wsu.edu

Geng Yuan

Northeastern University  
Boston, MA, USA  
yuan.geng@northeastern.edu

Wei Niu

College of William and Mary  
Williamsburg, VA, USA  
wniu@email.wm.edu

Jiannan Tian

Washington State University  
Pullman, WA, USA  
jiannan.tian@wsu.edu

Sian Jin

Washington State University  
Pullman, WA, USA  
sian.jin@wsu.edu

Donglin Zhuang

University of Sydney  
Sydney, NSW, Australia  
dzhu9887@sydney.edu.au

Zhe Jiang

University of Alabama  
Tuscaloosa, AL, USA  
zjiang@cs.ua.edu

Yanzhi Wang

Northeastern University  
Boston, MA, USA  
yanz.wang@northeastern.edu

Bin Ren

College of William and Mary  
Williamsburg, VA, USA  
bren@cs.wm.edu

Shuaiwen Leon Song

University of Sydney  
Sydney, NSW, Australia  
shuaiwen.song@sydney.edu.au

Dingwen Tao\*

Washington State University  
Pullman, WA, USA  
dingwen.tao@wsu.edu

## ABSTRACT

Convolutional neural networks (CNNs) are becoming increasingly deeper, wider, and non-linear because of the growing demand on prediction accuracy and analysis quality. The wide and deep CNNs, however, require a large amount of computing resources and processing time. Many previous works have studied model pruning to improve inference performance, but little work has been done for effectively reducing training cost. In this paper, we propose **CLICK-TRAIN**: an efficient and accurate end-to-end training and pruning framework for CNNs. Different from the existing pruning-during-training work, **CLICK-TRAIN** provides higher model accuracy and compression ratio via fine-grained architecture-preserving pruning. By leveraging pattern-based pruning with our proposed novel accurate weight importance estimation, dynamic pattern generation and selection, and compiler-assisted computation optimizations, **CLICK-TRAIN** generates highly accurate and fast pruned CNN models for direct deployment without any extra time overhead, compared with the baseline training. **CLICK-TRAIN** also reduces the end-to-end time cost of the pruning-after-training method by up to 2.3 $\times$  with comparable accuracy and compression ratio. Moreover, compared with the state-of-the-art pruning-during-training approach, **CLICK-TRAIN** provides significant improvements both accuracy and compression ratio on the tested CNN models and datasets, under similar limited training time.

## ACM Reference Format:

Chengming Zhang, Geng Yuan, Wei Niu, Jiannan Tian, Sian Jin, Donglin Zhuang, Zhe Jiang, Yanzhi Wang, Bin Ren, Shuaiwen Leon Song, and Dingwen Tao. 2021. ClickTrain: Efficient and Accurate End-to-End Deep Learning

\*Corresponding author: Dingwen Tao, School of Electrical Engineering & Computer Science, Washington State University, Pullman, WA 99163, USA.

Permission to make digital or hard copies of part or all of this work for personal or classroom use is granted without fee provided that copies are not made or distributed for profit or commercial advantage and that copies bear this notice and the full citation on the first page. Copyrights for third-party components of this work must be honored. For all other uses, contact the owner/author(s).

ICS '21, June 14–17, 2021, Virtual Event, USA

© 2021 Copyright held by the owner/author(s).

ACM ISBN 978-1-4503-8335-6/21/06.

<https://doi.org/10.1145/3447818.3459988>

Training via Fine-Grained Architecture-Preserving Pruning. In *2021 International Conference on Supercomputing (ICS '21)*, June 14–17, 2021, Virtual Event, USA. ACM, New York, NY, USA, 12 pages. <https://doi.org/10.1145/3447818.3459988>

## 1 INTRODUCTION

Deep neural networks (DNNs) such as CNNs have rapidly evolved to the state-of-the-art technique for many artificial intelligence (AI) tasks in various science and technology areas, such as image and vision recognition [41], recommender systems [44], natural language processing [7]. DNNs contain millions of parameters in an unparalleled representation, which is efficient for modeling complexity nonlinearities. Many works [16, 21, 43] have suggested that using either deeper or wider DNNs is an effective way to improve analysis quality, and in fact many recent DNNs have gone significantly deeper and/or wider [20, 45]. For instance, OpenAI recently published their new DNN-based NLP model GPT-3 [4] with 175 billion parameters, which is the largest NLP model that is ever trained. Compared with its predecessor GPT-2, GPT-3 expands the capacity by three orders of magnitudes without significant modification to the model architecture, instead just adopting deeper and wider layers [4].

The ever-increasing scale and complexity of the networks with large-scale training datasets such as ImageNet-2012 [22] are bringing more and more challenges to the cost of DNN training, which requires large amounts of computations and resources such as memory, storage, and I/O. Moreover, designing new DNN architectures and training algorithms for various AI tasks require numerous trial-and-error and fine-tuning processes, which makes the training cost issue worse and computing resources scarce.

Model pruning is a widely used approach to reduce the number of DNN weights, which can effectively reduce the computation and storage costs and increase the inference performance, especially for resource-limited platforms, such as mobile, edge, and IoT devices. Many model pruning works have been proposed for improving the performance and energy efficiency of DNN inference [15, 26, 34, 47, 51]. A typical procedure to prune a DNN model consists of ① training a model to high accuracy, ② pruning the

well-trained model, and ③ fine-tuning the pruned model. However, this procedure (called *pruning-after-training* or *PAT*) often requires a well-trained model and a trial-and-error process with domain expertise, which is typically very time-consuming. For example, state-of-the-art PAT-based methods [29, 31] incorporate the alternating direction method of multipliers (ADMM) into the pruning process to achieve high compression ratio and accuracy, but they almost triple the overall training time.

Considering the weights of DNN models are gradually sparsified during training, combining the pruning and training phases together (called *pruning-during-training* or *PDT*) is a promising way to significantly reduce the end-to-end time cost<sup>1</sup> and conserve computing resources. However, only few work has investigated how to prune DNN models during training while still achieving highly accurate and fast pruned models that can be directly deployed.

Recently, a state-of-the-art work PRUNETRAIN [27] studied how to perform CNN pruning during training. PRUNETRAIN adopts a group-lasso regularization ( $\ell_1$ -based regularization) [32] to gradually force a group of model weights with small magnitudes to zero and periodically reconfigure the CNN architecture (e.g., reducing the number of layers) during training, leading to lower computation and higher performance. However, in reality, adaptively changing the original network architecture may result in severe loss of accuracy, which cannot be compensated for by performing more training batches. Thus, how to design a PDT-based method to significantly reduce the end-to-end time while still maintaining the network architecture for high accuracy remains an open question.

In this paper, we propose CLICKTRAIN—a fast and accurate integrated framework for CNN training and pruning—which significantly reduces the end-to-end time. We develop a series of algorithm-level and system-level optimizations for CLICKTRAIN to achieve high computation efficiency toward highly accurate and fast pruned models for inference. The key insights explored for algorithm-level optimization include: ① the position of the most important weight in each convolution kernel is relatively stable after certain training batches, and ② the important weights tend to be adjacent to each other. Thus, we propose a fine-grained architecture-preserving pruning approach based on pattern-based pruning (will be discussed in §2.1), which can preserve the original training accuracy under a higher compression ratio. Moreover, our optimized pattern-based pruning creates multiple opportunities for system-level optimization such as sparse convolution acceleration and communication (Allreduce) optimization for weight update assisted by compiler so that the time overhead introduced by our proposed regularization can be mitigated. To the best of our knowledge, our paper is *the first work to study how to design a PDT-based approach for effectively reducing the end-to-end time cost while achieving very high accuracy and compression ratio of pruned models*. The main contributions are listed below:

- Instead of commonly used weight selection methods based on magnitude, we incorporate a state-of-the-art weight importance estimation approach to select the desired patterns from a generated candidate pattern pool. Moreover, we propose methods to gradually generate the candidate patterns

(called *dynamic pattern pool generation*) and adaptively finalize the patterns and unimportant kernels.

- We propose a modified group-lasso regularization to replace the expensive ADMM method for pattern-based pruning.
- We propose multiple system-level optimizations including fast sparse matrix format conversion, pattern-accelerated sparse convolution, pattern-based communication optimization, and compiler-assisted optimized code generation, to significantly accelerate CLICKTRAIN by leveraging finalized pattern sparsity during the training.
- We compare CLICKTRAIN with state-of-the-art PAT-/PDT-based methods. Experiments illustrate that CLICKTRAIN can generate highly accurate and fast pruned models for direct deployment without any extra time overhead or even faster, compared with the baseline training. Meanwhile, CLICKTRAIN significantly reduces the training time of PAT-based approaches by up to about 2.3× with comparable accuracy and compression ratio, and improves the accuracy and compression ratio by up to 2.0% and 4.9× over PRUNETRAIN.

The rest of the paper is organized as follows. We present background information in §2. We discuss our research motivation and challenges in §3. We describe our algorithm-level design and system-level optimizations of CLICKTRAIN in §4 and §5, respectively. We present our evaluation results in §6. We discuss related work and conclude our work in §7 and §8.

## 2 BACKGROUND

### 2.1 DNN Model Pruning

Weight pruning for DNN model compression has been well studied in recent years. Below are three main methods.

**Non-Structured Pruning.** The non-structured pruning methods studied in the previous works [53] aim to heuristically prune the redundant weights on arbitrary locations. This leads to irregular weight distribution and inevitably introduces extra indices to store the locations of pruned weights. Eventually, this drawback limits performance acceleration [9].

**Structured Pruning.** To overcome these limitations, structured pruning has been investigated in the recent studies [17, 18, 27]. They proposed to prune the entire filters, channels to maintain the structural regularity of the weight matrices after pruning. By taking advantage of the regular shapes of the pruned weight matrices, structured pruning becomes more hardware-friendly and achieves much higher speedups [30]. However, due to the constraints of its coarse-grained pruning, structured pruning suffers from high accuracy loss.

**Fined-Grained Pattern-Based Pruning.** The state-of-the-art pruning work [36] proposes a fine-grained pattern-based pruning scheme, which generates an intermediate sparsity type between non-structured pruning and structured pruning. They prune a fixed number of weights in each convolution kernel (e.g., pruning 5 weights out of 9 weights in a 3×3 convolution kernel), and make the remaining weights to be concentrated in a certain area to form specific kernel patterns (called *pattern sparsity*), as shown in Figure 1 (left). However, the compression ratio that is achieved by

<sup>1</sup>End-to-end time refers to the total time from the beginning of training from scratch to the end of pruning with a ready-to-deploy model.

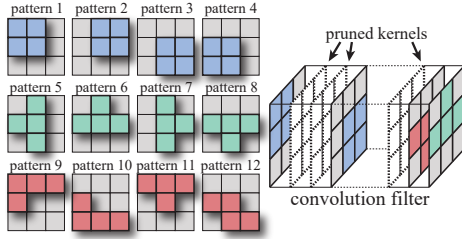


Figure 1: Pattern-based pruning with pruned kernels.

pattern sparsity is limited. So, they further propose to exploit the inter-convolution kernel sparsity, which aims to remove some unimportant kernels (called *connectivity sparsity*), as shown in Figure 1 (right). It can further enlarge the weights compression rate while reducing the convolution operations in CNNs.

The pattern-based pruning emphasizes exploiting locality in layer-wise computation, which is prevalent and widely reflected in the domains like human visual systems [13]. Moreover, this approach is more flexible that leads to a higher model accuracy compared to the prior coarse-grained filter/channel pruning schemes [27, 52]. Overall, a fine-grained pattern-based pruning approach, as state-of-the-art pruning scheme, considering both pattern and connectivity sparsity can leverage the advantages of non-structured and structured pruning to make the trade-off among regularity, accuracy, and compression ratio.

## 2.2 Pruning-after-training (PAT) Versus Pruning-during-training (PDT)

GBN [50], GAL [23] and DCP [54] are three state-of-the-art PAT-based approaches. GBN and GAL mainly focus on pruning filters. DCP accelerates the CNN inference via channel pruning. However, all of them must need well-trained models to converge to an accurate pruned model with high compression ratio, which suffers from high time cost, compared with PDT-based approaches.

PRUNETRAIN [27] is a state-of-the-art PDT-based approach. The work observed that when pruning with group-lasso regularization, once a group of model weights are penalized close to zero, their magnitudes are typically impossible to recover during the rest of the training process. Based on this, PRUNETRAIN periodically removes the small weights and change the network architecture and hence gradually reduces the training cost toward high compression ratio and accuracy. Moreover, NEST [8] and TAS [10] are two state-of-the-art methods attempting to search the best-fit pruned network architecture during training (can be seen as PDT-based methods), but they suffer from extremely high time cost.

## 3 MOTIVATION AND CHALLENGES

### 3.1 Limitations of Existing PDT-based Method

The state-of-the-art PDT-based approach PRUNETRAIN [27] integrates the structured pruning with group-lasso regularization ( $\ell_1$ -based regularization) [32] into the training phase, which is designed to prune as many channels, filters, and layers as possible to acquire a compact architecture with relatively high training performance. However, there are two major challenges to deploy PRUNETRAIN for training large neural networks on a variety of architectures: inferior validation accuracy and large storage overhead.

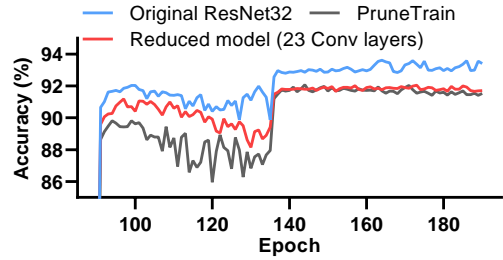


Figure 2: Achieved accuracies with three strategies: full training, PRUNETRAIN, training on reduced architecture.

**Inferior Validation Accuracy.** PRUNETRAIN saves the training floating-point operations (FLOPs) by drastically reconfiguring the original network architectures (e.g., reducing the depth), resulting in a notable accuracy loss for many network architectures. For example, PRUNETRAIN can save 53% training FLOPs and 66% inference FLOPs (i.e., about 2.2 $\times$  compression ratio) but cause 1.8% accuracy drop for ResNet-34 on the CIFAR-10 dataset. Moreover, for demonstration purposes, we compare three different training strategies on ResNet-34, including (1) normal full training from scratch on the original ResNet-34 model, (2) PRUNETRAIN for training the original 34-layer ResNet, and (3) training from scratch using an identical network structure as the one generated from PRUNETRAIN (i.e., 23 CONV layers). As shown in Figure 2, PRUNETRAIN achieves a lower model accuracy compared to training on the reduced model, but both of them cannot reach the expected accuracy of the original ResNet-34 network, even though we train for an extra of 1,000 epochs. This experiment illustrates that the accuracy is highly relevant to network architectures. Moreover, studies [10, 11, 16, 24] demonstrate that the model accuracy is highly relevant to network architecture, thus, we conclude that *aggressively preserving the original architecture is critical to prevent a notable accuracy drop*.

**Large Storage Overhead.** One major purpose of pruning large-scale neural networks is to facilitate their deployments in resource-constrained computing platforms which suffer from limited storage capacity and computing power. Thus, to realistically alleviate the storage and computation burden, pruning must provide a high compression ratio. However, PRUNETRAIN can only provide up to 3 $\times$  compression ratio (e.g., 2.2 $\times$  for ResNet-34) [27], which is far below the expectation.

Therefore, these issues motivate us to develop a solution that provides *three-dimensional optimizations*: high training efficiency, high compression ratio, and high model accuracy.

### 3.2 Challenges of Pattern-based Pruning in Training

Recent works [31, 36] have applied pattern-based pruning techniques for improving inference efficiency. However, these inference-focused strategies will pose several challenges to reach our three optimization objectives.

**Issues of Existing Pattern Pruning Algorithms.** There are three main issues of the existing pattern-based pruning algorithms [9, 36]: (1) The existing algorithms select pattern for each kernel via estimating weight importance based on magnitude. However, this estimation approach requires a well-trained model, whose

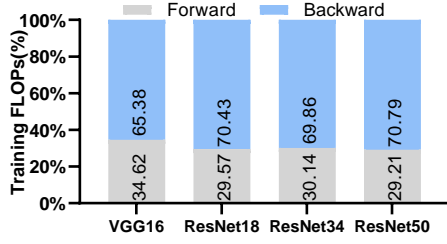


Figure 3: Percentage of floating-point operations in forward and backward phases with different CNN models.

weights will not change dramatically, *which is not true for training from scratch*. (2) The existing algorithms predefine the candidate patterns for all kernels and statically select the best-fit pattern for each kernel. But for pruning during training, static patterns may not work properly, resulting in a significant loss of accuracy. (3) The existing algorithms typically with ADMM-based methods are very time-consuming and not applicable for training acceleration.

**Lack of Training Efficiency Optimization.** The computation efficiency optimizations proposed by existing works [9, 36] for pattern-based pruning cannot be directly applied to our training framework. This is mainly because of two reasons. On one hand, the existing pattern-based acceleration techniques [9, 36] are designed for accelerating inference (i.e., forward phase) instead of training (including both forward and back phases). However, based on our profiling result as shown in Figure 3, backward phase can consume more than 70% of the overall training FLOPs. On the other hand, the existing pattern-based optimizations [36] are based on accelerating numerous convolution operations on embedded systems due to limited memory capacity. However, efficient training on advanced datacenter architectures relies on high-performance general matrix-matrix multiplication (GEMM) rather than a large number of convolutions, in order to leverage the high throughput of accelerators such as GPUs. Thus, there is an urgent need for an effective method to take advantage of pattern-based pruning to improve the GEMM-based convolution computation efficiency.

Overall, these challenges demand a novel solution that can provide both *algorithm-level* and *system-level* supports for fast and accurate end-to-end training toward our three objectives.

## 4 ALGORITHM-LEVEL DESIGN OF CLICKTRAIN

In this section, we propose our novel PDT-based framework called CLICKTRAIN. The overall framework flow is shown in Figure 4, which consists of five stages. In this section, we focus on the algorithm-level design of CLICKTRAIN (used in stage 2 to stage 4) mainly for quickly obtaining the model with desired pattern-based sparsity. We first propose our pattern selection using weight importance estimation. Next, we propose our methods to dynamically build up the pattern candidates and adaptively finalize the patterns and unimportant kernels. After that, we describe our modified group-lasso regularization to accurately penalize the weights outside of the selected patterns and the unimportant kernels.

### 4.1 Pattern and Kernel Selection Criterion

**Weight importance estimation.** The key consideration in the pattern-based pruning is to select the best-fit pattern for each kernel

after appropriately designing the patterns. The previous methods [28, 36] determine the importance of a certain weight based on its magnitude, which requires a well-trained CNN model whose weights will not change dramatically and well distributed after pruning the redundant filters. However, it is not feasible to accurately determine the importance of a certain weight only based on its weight magnitude during training from scratch because *the weights in a not well-trained model will change greatly*, especially in the early training. Therefore, we propose to estimate the importance of patterns by further considering gradient information and to select the most important pattern for each kernel in the pruning.

For a given CNN with  $L$  convolutional layers, let  $W^{(\ell)}$  ( $1 \leq \ell \leq L$ ) denote the collection of weights for all the kernels in convolutional layer  $\ell$ , which forms a 4-D tensor  $W^{(\ell)} \in \mathbb{R}^{F_\ell \times C_\ell \times H_\ell \times S_\ell}$ , where  $F_\ell, C_\ell, H_\ell, S_\ell$  are the dimensions for the axes of filter, channel, spatial height, spatial width, respectively. As suggested by [33], for a weight  $w_m \in W^{(\ell)}$ , its importance can be estimated by  $(g_m w_m)^2$ , where  $g_m = \frac{\partial E(W, D)}{\partial w_m}$  is the gradient of the weight  $w_m$ . Here  $E(W, D)$  is the loss function on the dataset  $D$ . In addition,  $W$  represents the collection of all 4-D weight tensors for  $L$  convolutional layers.

A pattern  $p_i$  (where  $p_i \in B$  is the  $i$ -th pattern from the candidate pattern pool  $B = \{p_1, p_2, \dots, p_N\}$ ) can be viewed as a mask to prune specific weights within a kernel. The remaining weights of the kernel form a certain pattern. Thus, we can estimate the importance score of a pattern  $p_i$  by combining the importance scores of all the remaining weights. We will discuss how to *gradually generate the pattern pool* in the next section. The patterns corresponding to the convolutional layer  $\ell$  also form a 4-D tensor  $P^{(\ell)} \in \mathbb{R}^{F_\ell \times C_\ell \times H_\ell \times S_\ell}$ , where  $P_{f_\ell, c_\ell, :, :}^{(\ell)} \in B$ . The importance score of  $p_i$  is estimated as

$$t_{:, :} = G_{f_\ell, c_\ell, :, :}^{(\ell)} \odot W_{f_\ell, c_\ell, :, :}^{(\ell)} \odot p_i, \quad I_{p_i} = \sum_{h_\ell} \sum_{s_\ell} (t_{h_\ell \times s_\ell})^2, \quad (1)$$

where  $G^{(\ell)}$  denotes the 4-D gradient tensor corresponding to  $W^{(\ell)}$  and  $\odot$  is the element-wise product (a.k.a. Hadamard product). After assessing the importance of all the patterns for a kernel, we can choose the pattern with the highest estimated importance score as the best-fit pattern for this kernel.

In addition, to further enlarge the sparsity, we also need to determine the unimportant kernels and directly prune them (i.e., connectivity sparsity). We adopt the following equation to estimate the importance score of a kernel  $k_i \in W^{(\ell)}$ .

$$t_{:, :} = G_{f_\ell, c_\ell, :, :}^{(\ell)} \odot W_{f_\ell, c_\ell, :, :}^{(\ell)}, \quad I_{k_i} = \sum_{h_\ell} \sum_{s_\ell} (t_{h_\ell \times s_\ell})^2. \quad (2)$$

The reason why we integrate gradient to estimate the importance is if a certain weight whose magnitude and gradient are small, it will very likely keep the small value in the following training process because the backpropagation tends not to update its value dramatically. Therefore, we can treat it as an unimportant weight and penalize such weights during training to push it to become smaller and smaller (less and less important). Eventually, we can prune it with no hurt to the final accuracy. The computation cost of Equation (1) and (2) are relatively low, since the gradient  $G^{(\ell)}$  can be acquired in the backward-propagation stage, which can be naturally implemented in most of the deep learning frameworks

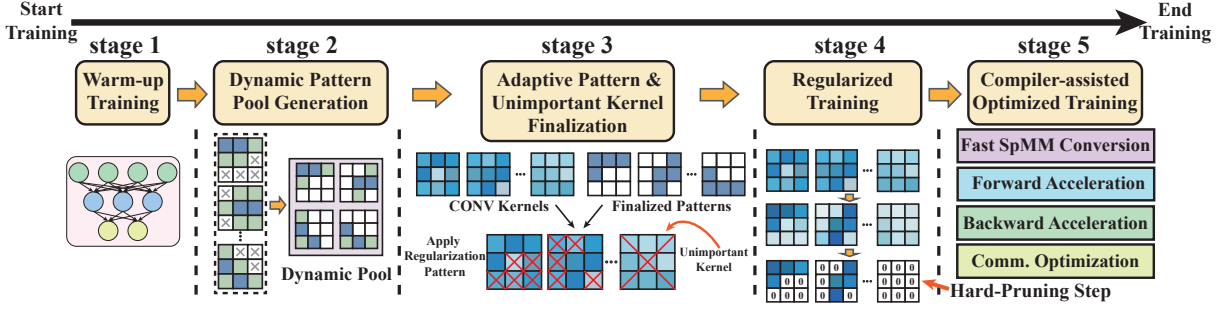


Figure 4: Overview of our proposed fast and accurate end-to-end deep learning training framework CLICKTRAIN.

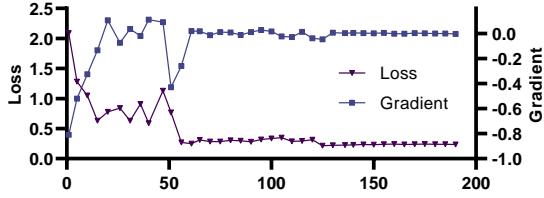


Figure 5: Loss & gradient in training ResNet-34 on CIFAR-10.

[2, 39]. Moreover, the number of candidate patterns is limited to a relatively small number (will be discussed later).

**Pattern and kernel selection.** The weights and gradients would change greatly during the first few epochs of training CNN. On one hand, estimating the weight importance earlier can help us remove these unimportant weights sooner, thereby reducing the overall training time. On the other hand, estimating the importance of weights prematurely will lead to inaccurate estimations and ultimately cause a significant accuracy drop. Later estimation does help to improve the pruning accuracy but would cost more training epochs. Therefore, when we should apply the formulas above to accurately assess the weight importance is a challenge to address. After a series of empirical evaluation, we conclude that *the derivative of the loss function on epochs can be used as a good indicator to solve this problem*. In particular, when this value is less than a threshold, we can apply the formula above to evaluate the weight importance relatively accurately. For example, Figure 5 shows that the loss does not change sharply after a certain threshold (50 epochs), meaning that the optimization process gradually stabilizes to start our pruning.

## 4.2 Dynamic Pattern Pool Generation

**Limitations of static pattern pool.** As discussed in Section 2.1, using  $3 \times 3$  kernel as an example, a pattern can be formed by any 4 positions inside a kernel, which will result in a total number of  $\binom{9}{4} = 126$  possible different pattern types. In general, a larger number of pattern types used in a CNN will lead to a considerable runtime overhead, offsetting the training acceleration. On the other hand, too few pattern types will reduce the pruning flexibility and hence accuracy degradation. To preserve a high accuracy while not compromising computation efficiency, we need to limit the number of candidate pattern types that can be used for pruning.

Moreover, unlike pruning a well-trained CNN, pruning during training faces the challenge that the positions of importance weights are not stabilized. It is not ideal to determine the positions of pruned weights only once and fix them in the subsequent training process.

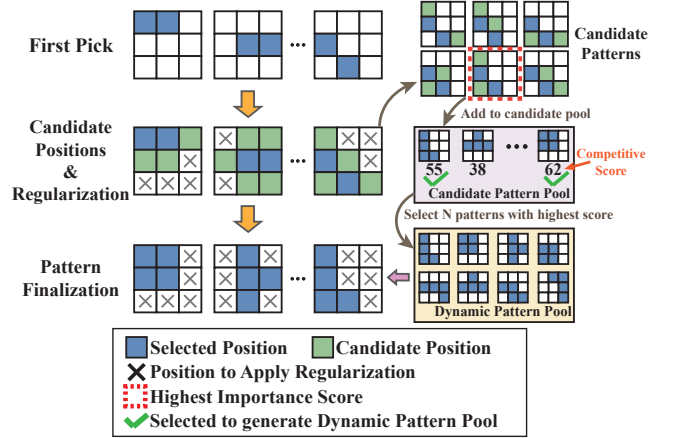


Figure 6: Our proposed DPPG method.

Therefore, we propose the Dynamic Pattern Pool Generation (DPPG) method, which selects important weights gradually to build a pattern pool with a limited number of desired pattern types. A multi-stage procedure is proposed to build pattern pool dynamically. In this work we use  $3 \times 3$  kernels for demonstration, but our proposed method can also be applied to other kernel sizes, such as  $5 \times 5$ ,  $7 \times 7$ .

**Proposed dynamic pool generation process.** The whole process mainly consists of the following six steps. ① We first select one weight position with the highest estimated importance score in each kernel. ② We then select the second weight position with the highest importance score among the adjacent positions of the first position, including its horizontal, vertical, and diagonal adjacent position. ③ After determining the first two positions in patterns (marked in blue in Figure 6), we mark the adjacent positions to the first two positions as the “candidate positions” (marked in green). ④ For each kernel, we pick two candidate positions together with the first two positions to form a candidate pattern. We evaluate the importance score (as mentioned in Section 4.1) of all possible combinations (i.e., candidate patterns) to find the candidate pattern with the highest score, then add it to a global candidate pattern pool. Each candidate pattern in the candidate pattern pool has a competitive score that is initialized to 1. If the candidate pattern already exists in the candidate pattern pool, then we add “1” to its competitive score. ⑤ We repeat the step 1~4 for a certain number of epochs (depending on the training epoch budget), and keep accumulating the competitive scores in the candidate pattern pool. ⑥ Finally, we obtain the desired final pattern pool by selecting  $N$  candidate patterns from candidate pattern pool with the highest



competitive scores, where  $N$  is the given number of total pattern types (usually is set to 8 or 12).

**Detailed optimizations.** In order to better cluster the candidate patterns in the candidate pattern pool and generate a desired pattern pool, we apply several optimizations/constraints during the dynamic pattern pool generation process.

For ②, the selection rule of the second weight position is derived by considering two observations: i) the position of the most important weight (i.e., the highest-scoring weight) in each kernel is relatively stable after certain training iterations, and ii) the weight distribution in unpruned (dense) well-trained models suggest that the important weights tend to be adjacent to each other.

For ③, since the weights on the candidate positions are usually less important than the firstly selected two weights, model has a higher tolerance for these weights not being selected optimally. Thus, we intentionally exclude the diagonal adjacent positions to reduce the diversity of the candidate positions to cluster the candidate patterns. Moreover, by limiting the possible candidate positions in ③, part of the pruning positions (marked as “x” in Figure 6) in each kernel can be determined earlier, thereby starting the regularization and fine tuning sooner, which both reduces the training time and enhances the pattern formation process.

### 4.3 Adaptive Pattern and Kernel Finalization

After the pattern pool is generated, we can finalize the pattern for each kernel adaptively based on the pattern pool. Due to the concern that the one-time selection method may not provide high accuracy, we propose an adaptive method to finalize the patterns using multiple training epochs. Specifically, in each training batch, for every kernel, we calculate the importance score of each pattern in our pattern pool. Then, we find the pattern with the highest importance score and count its number of occurrences during training. After a number of epochs, the final pattern for each kernel will be selected as the most frequent one of those highest-scoring patterns.

Similarly, we also use our importance estimation method to calculate the importance score for each kernel and adaptively select a user-set number of unimportant kernels for each layer. Note that the loss is not always decreasing during training. Thus, we set up a training loss margin  $\delta$  as a hyperparameter to avoid selecting patterns in the training batches where the loss is obviously increasing. For example, if the loss in the previous batch divided by the value in the current batch is smaller than 0.0018 (default  $\delta$ ), we will not count the highest-scoring patterns into the number of occurrences. In addition, Figure 8 illustrates that 12 dynamic patterns achieves 2% higher than the one-time solution on CIFAR-10 since kernels have greater probability of selecting the appropriate pattern.

### 4.4 Modified Group Lasso Regularization

$\ell_1$ -based regularization or group-lasso regularization is usually added to the loss function to penalize all important or unimportant weights along desired dimensions (such as filter, channel) over the entire layers of CNNs. However, we have noted that using group-lasso regularization to penalize all the weights of filters or channels can lead to a *severely impaired pruned model*. Thus, we propose a modified group-lasso regularization to more accurately penalize the weights. Generally speaking, unimportant weights

should be punished more heavily than important weights, and important weights should remain the same because they typically play a key role in generating stronger activation to make more confident decisions. In particular, after selecting the best-fit pattern for each kernel and identifying the unimportant kernels, we only penalize the unimportant kernels and the weights outside of the selected patterns, since we desire to reduce the absolute values of these weights and kernels as the training progresses. We note that the contributions of these weights/kernels to the final accuracy are negligible, so even if we directly remove (i.e., hard prune) these weights/kernels, the model accuracy would not decrease obviously.

Let  $I^{(\ell)}$  be a 4-D importance tensor (i.e., a tensor full of importance scores) of a 4-D weight tensor  $W^{(\ell)}$ , where  $I^{(\ell)}$  is the same shape as  $W^{(\ell)}$ . Assume the  $c_\ell$ -th kernel of the  $f_\ell$ -th filter in the convolutional layer  $\ell$  is unimportant, we set  $I_{f_\ell, c_\ell, :, :}^{(\ell)}$  to be 0. Our proposed approach for penalizing unimportant weights and kernels with modified group-lasso regularization can be formulated as:

$$\begin{array}{|l|l|} \hline Z^{(\ell)} = W^{(\ell)} \odot (-P^{(\ell)}), & E(W, D) = E(W, D) \\ U^{(\ell)} = W^{(\ell)} \odot (-I^{(\ell)}), & + \lambda_P \sum_{f=1}^L \left( \sum_{f_\ell=1}^{F_\ell} \sum_{k_\ell=1}^{K_\ell} \|Z_{f_\ell, k_\ell, :, :}^{(\ell)}\|_g \right), \\ \hline \end{array}$$

where  $\|w^{(g)}\|_g = \sqrt{\sum_{i=1}^{|w^{(g)}|} (w_i^{(g)})^2}$ ,  $|w^{(g)}|$  is the number of weights in  $w^{(g)}$ ,  $-$  is the element-wise inversion operator (i.e.,  $0 \rightarrow 1$  or  $1 \rightarrow 0$ ), and  $\lambda$  is the coefficients for the group-lasso regularization. Here the inverse tensors  $-P^{(\ell)}$  and  $-I^{(\ell)}$  can be considered as masks, which can prevent from unnecessarily penalizing the important weights. Moreover, these tensor operations can be accelerated by many popular GPU-based deep learning frameworks such as TensorFlow and PyTorch [2, 39] to speedup the group lasso.

## 5 SYSTEM-LEVEL OPTIMIZATIONS OF CLICKTRAIN

In this section, we discuss our proposed system-level optimizations (used in stage 5) for improving training computation efficiency.

### 5.1 Pattern-driven Fast Sparse Matrix Conversion

Kernels become much more sparse than origins after pruning. According to prior studies [5, 48], a highly optimized sparse matrix-matrix multiplication (SpMM) leveraging pruning sparsity can outperform state-of-the-art GPU GEMM libraries such as cuBLAS [38] for convolution computation. SpMM typically requires converting dense input matrix to a sparse format such as Compressed Sparse Row (CSR) because CSR dominates a continuous storage space, which is beneficial to data locality and computation efficiency.

However, converting a dense matrix to its CSR format (as shown in Figure 7 (a)) usually introduces an obvious time overhead if directly calling `dense2csr()` from cuSPARSE library [35]. For example, as shown in Figure 9, `dense2csr()` costs about 800 us when converting a  $256 \times 1152$  dense matrix to its CSR format (generated by the convolution operation on  $128 \times 224 \times 224$  and  $256 \times 3 \times 3$  tensors), whereas the time of the corresponding SpMM of  $256 \times 1152$  (sparse) multiplying  $1152 \times 50176$  (dense) is only about 3000 us. We note that after the patterns have been finalized, the positions of un-pruned

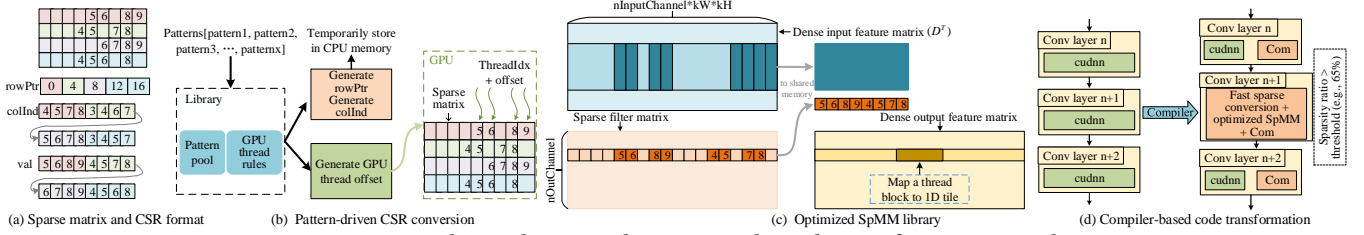


Figure 7: Our proposed compiler-assisted pattern-accelerated SpMM for sparse convolution.

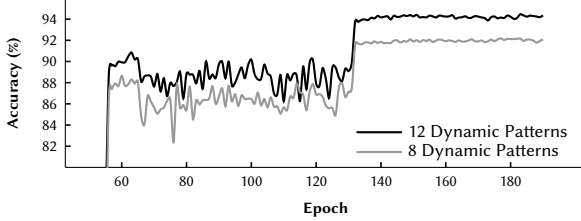


Figure 8: Accuracy comparison between 8 and 12 dynamic patterns.

(non-zero) weights will not change. Thus, we can directly generate rowPtr, colInd, and GPU thread offset arrays (as shown in Figure 7 (b)) during stage 3 (as shown in Figure 4) and store them for the following SpMM-based convolution operations. Note that this indices generation only introduces a negligible time overhead, since we only need to generate the fixed arrays for once and keep using them in the next stages.

Moreover, since dense2csr() does not provide any interface for pre-defined nonzero positions (rowPtr and colInd), we propose a fast dense-to-sparse matrix conversion routine with pre-defined nonzero positions, whose interface as follow.

```
template <typename T> Convert2CSR(int* rowPtr, int* colInd, T* sparseFilters, T* val)
```

Note that in order to maintain a minimal modification to the existing popular deep learning frameworks such as PyTorch which uses dense matrices for most computations such as autograd (automatic differentiation), we apply our fast dense-to-sparse matrix conversion before each SpMM (for all filters in one layer) rather than changing all computations to be based on sparse matrices.

For demonstration purpose, we evaluate our proposed fast matrix conversion on the  $256 \times 1152$  and  $1152 \times 50176$  matrices using an NVIDIA RTX 5000 GPU and compare it with cuSPARSE. Figure 9 illustrates that our conversion implementation is 4 $\times$  faster than cuSPARSE’s dense2csr().

## 5.2 Pattern-Accelerated SpMM for Sparse Convolution

Ideally, we can save the floating-point operations if not involving the pruned weights (zeros) in the convolution operation. However, even though pattern sparsity is more regular than random sparsity (unstructured pruning), existing hardware such as GPUs cannot utilize the pattern sparsity to accelerate either forward or backward phase. We observe that our pattern sparsity exhibits three key characteristics: ① The types of sparsity is relatively limited, such as 4, 8, or 12. ② The non-zero (un-pruned) weights inside a kernel are more likely close to each other. ③ Each kernel has the same number of non-zero weights. Therefore, considering that SpMM

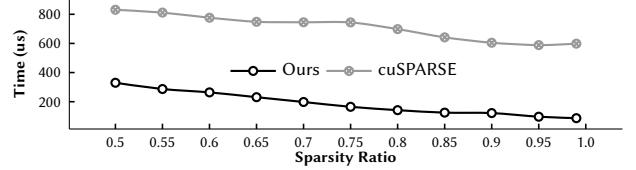


Figure 9: CSR conversion time.

can decrease the computational cost for sparse convolution operations by reducing the number of multiplications and additions, we propose to design a new GPU SpMM library for sparse convolution to make full use of the above important characteristics.

**Pattern-Accelerated SpMM.** We first describe our design of pattern-accelerated GPU SpMM library that exploits the pattern sparsity in both forward and backward phases. Specifically, converted sparse matrices after pruning lose the regular structure of dense matrices, which results in irregular memory accesses in SpMM. Moreover, concurrently executing massive threads on GPU makes the random memory access issue worse. Thus, improper handling of random memory accesses from massive parallel threads would stall the thread execution and decrease the performance significantly. In order to overcome the challenge of random memory accesses, we propose to take advantage of shared memory on GPU architectures to support concurrent random accesses. Specifically, we first load a tile of data from input feature matrix (dense) and filter matrix (sparse) to shared memory, as shown in Figure 7 (c). Then, we use the loaded data (in shared memory) to calculate the corresponding tile of output feature matrix (dense). Inspired by existing works [14, 19], load imbalance may severely hurt the performance on the GPU, while we solve this issue through an algorithm-hardware co-design. On the algorithm side, we limit all the filters in the same layer have the same number of un-pruned (non-zero) weights in our pattern-based pruning. On the hardware side, we can further improve the performance by using the vectorized load and store instructions in CUDA architectures [25] because each row of sparse filter matrix has the same length (i.e., non-zero weights). In addition, since the sparse matrices generated by convolution operations typically have relative long rows, we adopt 1D tiling strategy and map each thread block to a 1D

For demonstration purpose, we also evaluate our optimized SpMM on those  $256 \times 1152$  and  $1152 \times 50176$  matrices using an NVIDIA RTX 5000 GPU and compare it with state-of-the-art dense or sparse GEMM libraries. Figure 10 illustrates that our optimized SpMM library can achieve a speedup of 3.2 $\times$  over cuSPARSE. Moreover, our implementation is faster than cuBLAS’s GEMM and cuDNN’s convolution when the sparsity ratio is higher than 65%.

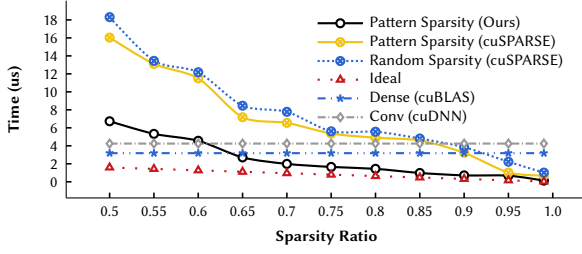


Figure 10: Convolution time with different methods.

**Forward Phase Acceleration.** To achieve a final high accuracy, the filters in different layers may have completely different compression/sparsity ratio. We note that for relatively low sparsity ratio, our optimized SpMM does not gain a performance improvement compared to its dense counterpart (will be showed later). Thus, we set a threshold of sparsity ratio for each layer, and only call our optimized SpMM for the layer where its sparsity ratio is higher than the threshold in the forward phase. Based on experiment, we set 65% as the default threshold for all layers without loss of generality.

**Backward Phase Acceleration.** The output  $z^\ell$  (before activate function  $\sigma$ ) of the convolutional layer  $\ell$  in the CNNs' forward-propagation is obtained by  $z^\ell = a^{\ell-1} \otimes W^\ell + b^\ell$ , where  $a^{\ell-1}$  is the activations at layer  $\ell - 1$ ,  $W^\ell$  and  $b^\ell$  denote weights and biases at layer  $\ell$ , respectively, and  $\otimes$  is the convolution operation. In backpropagation, the layer  $\ell$  first receives  $\delta^\ell$  from the layer  $\ell + 1$ , and then  $\delta^\ell$  is propagated back based on  $\delta^\ell = \frac{\partial E(W, D)}{\partial z^\ell}$ ,  $\delta^{\ell-1} = \delta^\ell \otimes \text{rot}180(W^\ell) \odot \sigma'(z^{\ell-1})$ . We can calculate the gradient of the layer  $\ell$  after obtaining  $\delta^\ell$  and  $\frac{\partial E(W, D)}{\partial W^\ell} = a^{\ell-1} \otimes \delta^\ell$ . We can observe from the above equation that the difference between forward and backward phases is that the forward phase uses feature map  $a^{\ell-1}$  as input, whereas the backward phase uses  $\delta^{\ell+1}$  as input. Also, the sparse weight matrix  $W^\ell$  is involved in the backpropagation, so we adopt the similar strategy as forward phase to handle  $W^\ell$ .

### 5.3 Communication Optimization

Distributed training has been widely used for large-scale DNN training. However, gradients must be synchronized among different computing nodes for each training batch, such communication (i.e., Allreduce) overhead is not negligible and will be scaled up as the number of computing nodes increases. Note that since all the weights to be pruned remain zeros after the regularized training stage, we do not need to send the corresponding gradients to other computing nodes in the rest of the training process. Moreover, high sparsity ratio of our pattern-based pruning provides a great opportunity to significantly reduce the communication overhead.

### 5.4 Compiler-Assisted Optimized Code Generation

After implementing our optimized libraries for sparse matrix conversion, SpMM, and Allreduce, we propose a compiler-assisted method to generate the optimized code for efficient training (in stage 5). Specifically, after sparsity ratios have been determined (after stage 3), the compiler decides whether using original sparse convolutions or our optimized SpMM computation for each layer in the computational graph based on its sparsity ratio; and accordingly generates the code with the better operator in the training

framework such as PyTorch (as shown in Figure 7 (d)). Moreover, the compiler transforms all Allreduce communications (in stage 5) in the computational graph into our optimized pattern-based communications. Note that there is an alternative solution that relies on compiler to generate the shared library calling sparse convolutions or SpMM computation dynamically for each layer. However, this solution introduces “if-else” overhead for each layer in every training batch, which is much higher than the former solution.

## 6 EXPERIMENTAL EVALUATION

In this section, we first evaluate our proposed CLICKTRAIN on different CNNs and datasets and show its accuracy and compression ratio and compare it with several state-of-the-art PDT-/PAT-based frameworks. We then evaluate our proposed optimizations and overall training efficiency on a single GPU and multiple GPUs.

### 6.1 Experimental Setup

We conduct our experimental evaluation using the Frontera supercomputer [42] at TACC, of which each GPU node is equipped with two Intel E5-2620 v4 CPUs and four NVIDIA Quadro RTX 5000 GPUs [1], interconnected by FDR InfiniBand. We use NVIDIA CUDA 10.1 and its default profiler for time measurement. We implement CLICKTRAIN based on PyTorch [39] using SGD. We evaluate CLICKTRAIN and compare it with state-of-the-art methods on seven well-known CNNs including ResNet18/34/50/101 and VGG11/13/16. Our datasets include CIFAR10/100 [6] and ImageNet-2012 [22]. Note that all accuracy shown in the following evaluation are based on the average of 10 experiments (variance lower than 0.2%).

Regarding hyperparameter, we initialize the learning rate as 0.1 and set the regularization penalty coefficient as 0.00025. The threshold in stage 1 used for determining when to start stage 2 is set to 0.27. The number of candidate patterns in stage 3 is set to 12, as suggested by Figure 8. We use the batch size (per GPU) of 128 and 64 for CIFAR and ImageNet, respectively.

### 6.2 Model Accuracy and Ratio Evaluation

We first evaluate our proposed CLICKTRAIN on different CNNs and datasets with a fixed number of training epochs, as shown in Table 1. We use  $\Delta$  to denote the validation accuracy drop of the pruned model compared to the original baseline model. Note that at the end of the regularized training stage, we conduct a hard-pruning step (as shown in Figure 4) to eventually zero out the pruned weights which have been regularized to tiny values. Thus, the rest of training process can be accelerated through our compiler-assisted training optimizations. We train the baseline models to a high accuracy using 190 epochs and 90 epochs for CIFAR10/100 and ImageNet, respectively. It is worth noting that all the above baseline accuracies have been widely used in many previous studies [27, 31, 36]. We thus use the same 190 epochs and 90 epochs for CLICKTRAIN on CIFAR and ImageNet, respectively. We calculate the compression ratio only considering the convolutional layers in the models, since the convolutional layers in ResNet and VGG models dominate most of the computation overhead in both training and inference processes. In particular, the compression ratio is calculated as  $\frac{\text{the total number of weights}}{\text{the total number of nonzero weights}}$  based on all the convolutional layers.



Table 1: Comparison between CLICKTRAIN (CLK) and PDT-based method PRUNETRAIN (PRT). FLOPs are the saved FLOPs.

		PDT Method	Base. Acc.	Valid. Acc. $\Delta$	Comp. Ratio	Train./Inf. FLOPs	Hard Pr. Epoch
CIFAR10	ResNet34	PRT	93.6%	-2.1%	2.2×	53% / 66%	N/A
		CLK	93.6%	0±0.05%	8.6×	39.2% / 79.2%	98
		CLK	93.6%	0±0.1%	10.7×	42% / 82.1%	95
	ResNet50	PRT	94.2%	-1.1%	2.2×	50% / 70%	N/A
		CLK	94.1%	0±0.06%	8.7×	37.4% / 74.9%	95
		CLK	94.1%	-0.2±0.05%	10.8×	41.6% / 79.1%	90
	VGG11	PRT	92.1%	-0.7%	6.6×	57% / 65%	N/A
		CLK	92.1%	-0.1±0.04%	8.6×	38.5% / 70%	96
		CLK	92.1%	-0.2±0.06%	10.2×	41.4% / 81.9%	94
	VGG13	PRT	93.9%	-0.6%	6.3×	56% / 63%	N/A
		CLK	93.8%	0±0.08%	7.2×	39.2% / 78.4%	95
		CLK	93.8%	-0.2±0.04%	9.1×	40.6% / 81%	96
CIFAR100	ResNet34	PRT	71.0%	-1.4%	1.8×	32% / 46%	N/A
		CLK	71.0%	0±0.05%	8.4×	36.5% / 77.3%	95
		CLK	71.0%	-0.2±0.05%	9.8×	39.7% / 80.7%	90
	ResNet50	PRT	73.1%	-0.7%	2.5×	53% / 69%	N/A
		CLK	73.1%	0±0.04%	8.3×	34.6% / 71.9%	96
		CLK	73.1%	-0.2±0.07%	11.0×	41.8% / 79.4%	95
	VGG11	PRT	70.6%	-1.3%	2.6×	47% / 57%	N/A
		CLK	70.6%	0±0.1%	8.9×	41.3% / 72.5%	95
		CLK	70.6%	-0.2±0.06%	9.8×	42.6% / 78.6%	92
	VGG13	PRT	74.1%	-1.4%	2.4×	42% / 52%	N/A
		CLK	74.1%	-0.1±0.08%	8.1×	39.7% / 80.3%	95
		CLK	74.1%	-0.3±0.07%	10.2×	41.7% / 82.3%	96
ImageNet	ResNet50	PRT	76.2%	-1.9%	2.1×	40% / 53%	N/A
		CLK	76.2%	-0.5±0.08%	4.1×	38.7% / 66%	43

Table 1 illustrates that for ResNet34 and ResNet50, our CLICKTRAIN can provide more than 10× compression ratio while maintaining up to 0.2% accuracy drop on the two CIFAR datasets, compared to the baseline accuracy. For VGG11/13, CLICKTRAIN can also provide 7.2× to 10.2× compression ratio with up to 0.3% accuracy drop. Since most of the weights in the convolutional layers have been pruned, CLICKTRAIN can save the training FLOPs and inference FLOPs by 39.7%~42.6% and 78.6%~82.3%, respectively, on CIFAR10/100 with the assist of compiler optimizations. To demonstrate the effectiveness on large dataset, we also train ResNet50 on ImageNet using CLICKTRAIN. It provides a compression ratio of 4.1× and saves the training/inference FLOPs by 38.7%/66%.

Note that the higher the compression ratio, the faster the inference of pruned model. For example, previous studies [36, 40] proved that for ResNet50 on ImageNet, a compression ratio of about 4.1 (as same as CLICKTRAIN’s) with the pattern-based pruning (adopted by CLICKTRAIN) reduces the model inference latency (batch size 1) by 9.8× on the Qualcomm Snapdragon 855 mobile platform (with a Qualcomm Kryo 485 octa-core CPU); in comparison, a previous work [46] illustrates that a compression ratio of about 2.1 (as same as PRUNETRAIN’s) with the structure pruning (adopted by PRUNETRAIN) reduces the inference latency by only 1.7× on an Intel Xeon E5-2680 v4 CPU. Note that the single-core performance difference between Kryo 485 and Xeon E5-2680 v4 is within 5% [37].

We also evaluate the impact of when to start the hard pruning on the validation accuracy and FLOPs. We observe that the earlier the patterns and unimportant kernels are determined, the earlier the models can be hard pruned by CLICKTRAIN, thus more training FLOPs can be saved; however, earlier hard pruning causes a significant accuracy loss. The epoch of hard pruning shown in Table 1 makes a good tradeoff between accuracy and training FLOPs.

Table 2: Comparison between CLICKTRAIN and PAT-based methods on ImageNet. Well-train costs about 90 epochs.

	PAT Method	Base. Acc.	Valid. Acc. $\Delta$	Comp. Ratio	Total Epochs
ResNet-18	TAS [10]	70.6%	-1.5%	1.5×	120
	DCP [54]	69.6%	-5.5%	3.3×	well train + 60
	CLK	69.9%	-0.7%	4.2×	90
ResNet-50	GBN [50]	75.8%	-0.6%	2.2×	well train + 60
	GAL [23]	76.4%	-7.1%	2.5×	well train + 30
	CLK	76.1%	-0.8%	4.1×	90
ResNet-101	Knapsack[3]	78.36%	-2.06%	3.5×	well train + 50
	CLK	79.32%	-1.5%	4.6×	90
VGG-16	NeST [8]	71.6%	-2.3%	6.5×	N/A
	CLK	73.1%	-0.8%	6.6×	90

**Comparison with PDT-based Method.** We then compare our CLICKTRAIN with the state-of-the-art PDT-based method PRUNETRAIN, as shown in Table 1. It illustrates that CLICKTRAIN can precisely control the accuracy drop within -0.3% for all the tested models on CIFAR10/100, but the accuracy drop of PRUNETRAIN is over -1.0% for most of the tested CNN models. Moreover, CLICKTRAIN can significantly improve the compression ratio with similar or even higher accuracy, compared to PRUNETRAIN. For example, PRUNETRAIN can only provide a compression ratio less than 3× with more than 1.0% accuracy drop for ResNet50 on CIFAR10, whereas CLICKTRAIN achieves 10.8× compression ratio with only 0.2% accuracy drop, leading to 4.9× higher compression ratio. For VGG13 on CIFAR100, PRUNETRAIN achieves 10.2× compression ratio with only 0.3% accuracy drop, which significantly outperforms PRUNETRAIN’s 2.4× compression ratio with 1.4% accuracy drop. For ImageNet, CLICKTRAIN reduces the accuracy drop by 1.3% and improves the compression ratio by 1.9× over PRUNETRAIN.

**Comparison with PAT-based Methods.** A typical procedure of model pruning is removing the redundant weights based on well-trained networks and then fine tuning the slashed networks. Thus, we finally compare our CLICKTRAIN with state-of-the-art PAT-based methods. As illustrated in Table 2, CLICKTRAIN save up to about 67% computation time while only sacrificing up to 0.8%

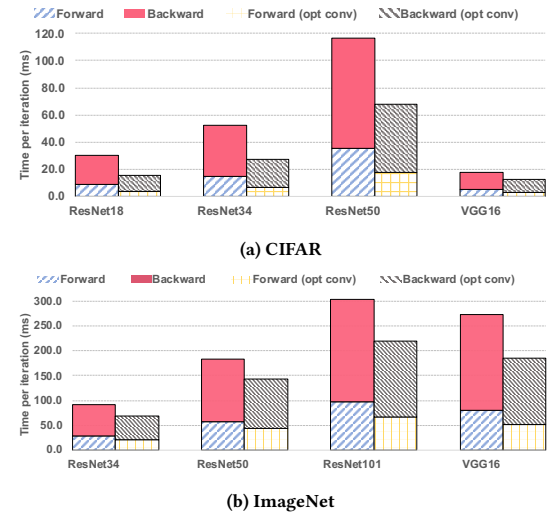


Figure 11: Average forward and backward time per iteration on CIFAR and ImageNet using a single GPU. “opt conv” means solution with our optimized SpMM for sparse convolution.

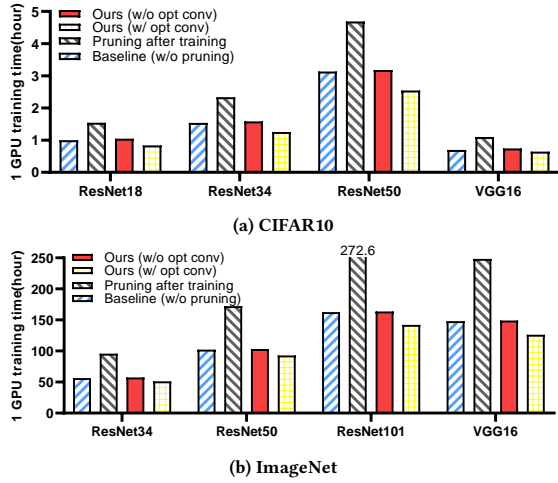


Figure 12: Total training time on CIFAR and ImageNet (single-GPU).

accuracy, compared with other PAT-based methods. In addition, CLICKTRAIN also achieves a much higher compression ratio for efficient inference. Thus, we conclude that accurately estimating the weight importance during training makes our PDT-based solution feasible to significantly save the total training epochs.

### 6.3 Single-GPU Performance Evaluation

Then, we evaluate the single-GPU performance gain by our PDT-based algorithm and optimized SpMM of CLICKTRAIN.

**Forward and Backward Acceleration.** We first evaluate the forward and backward time per iteration on a single GPU when applying our optimized SpMM using different CNN models with CIFAR and ImageNet. The sparsity (i.e., compression ratio) for each model can be found in Table 2.

Figure 11a shows that for forward phase on CIFAR, CLICKTRAIN achieves the speedups of 2.2 $\times$ , 2.1 $\times$ , and 1.9 $\times$ , and 1.6 $\times$  on ResNet18, ResNet34, ResNet50, and VGG16, respectively. For backward phase, CLICKTRAIN achieves the speedups of 1.8 $\times$ , 1.7 $\times$ , 1.6 $\times$ , and 1.3 $\times$  on ResNet18, ResNet34, ResNet50, and VGG16, respectively. Figure 11b shows that for forward phase on ImageNet, CLICKTRAIN achieves the speedups of 1.4 $\times$ , 1.3 $\times$ , 1.5 $\times$ , and 1.6 $\times$  on ResNet34, ResNet50, ResNet101, and VGG16, respectively. For backward phase on imagenet, CLICKTRAIN achieves the speedups of 1.3 $\times$ , 1.25 $\times$ , 1.35 $\times$ , and 1.5 $\times$  on ResNet34, ResNet50, ResNet101, and VGG16, respectively.

**Overall Training Acceleration.** We then evaluate the training acceleration of CLICKTRAIN with the four CNNs on CIFAR10 and ImageNet, as shown in Figure 12. Compared with the baseline training (i.e., training without pruning), CLICKTRAIN saves 0.16, 0.29, 0.59, and 0.15 hours on ResNet18/34/50 and VGG16, respectively, on CIFAR10. When training on ImageNet, CLICKTRAIN saves 5.1, 9.4, 20.4, and 19.7 hours on ResNet34/50/101 and VGG16, respectively.

### 6.4 Multi-GPU Performance Evaluation

**Communication Time.** Next, we evaluate our optimized communication time using multiple GPUs on ResNet50, ResNet101 and VGG16 with ImageNet, as shown in Figure 13. For ResNet50, CLICKTRAIN can save 23.9%, 26.3%, and 28.4% communication time per iteration using 4, 8, and 16 GPUs, respectively. For ResNet101,

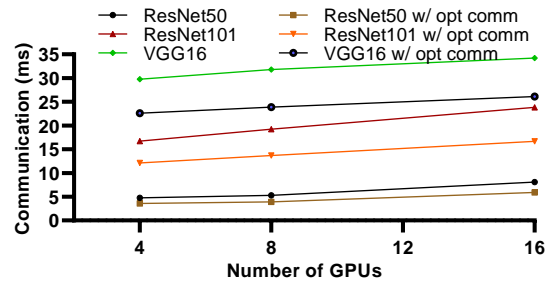


Figure 13: Communication time of baseline training and CLICKTRAIN with different numbers of GPUs. “opt comm” means solution with our optimized communication.

CLICKTRAIN can save 27.5%, 29.7%, and 31.2% communication time per iteration using 4, 8, and 16 GPUs, respectively. For VGG16, CLICKTRAIN can save 21.2%, 24.3%, and 24.9% communication time per iteration using 4, 8, and 16 GPUs, respectively. We notice that although PyTorch’s optimization of communication and computation overlap offsets our optimization for communication overhead to some extent, the performance gain will increase when increasing the scale (i.e., number of nodes and GPUs).

**Total Training Time.** Furthermore, we evaluate the overall training time on different CNN models using ImageNet with batch size 64 per GPU. Figure 14 shows that compared with the baseline training, for on ResNet50, CLICKTRAIN saves 3.2 hours, 2.1 hours, and 1.4 hours using 4, 8, and 16 GPUs, respectively; for ResNet101, CLICKTRAIN saves 7.1 hours, 4 hours, and 2.5 hours using 4, 8, and 16 GPUs, respectively; for on VGG16, CLICKTRAIN saves 6.3 hours, 4.6 hours, and 2.7 hours using 4, 8, and 16 GPUs, respectively. Note that unlike the baseline training, *CLICKTRAIN can generate ready-to-deploy models without further tuning such as pruning*. Moreover, compared with the baseline PAT-based approach (i.e., pattern-based pruning after training), CLICKTRAIN reduces the training time by  $1.67 \times / 1.96 \times / 2.13 \times$ ,  $1.86 \times / 1.99 \times / 2.18 \times$ , and  $1.98 \times / 2.15 \times / 2.25 \times$  using 4, 8, and 16 GPUs, respectively, on ResNet50/ResNet101/VGG16.

**Comparison with PatternTrain.** Finally, Figure 15a shows that CLICKTRAIN achieves a compression ratio of 10.8 $\times$  with only 0.1% accuracy drop on ResNet50 with CIFAR10, whereas PRUNETRAIN only has 2.2 $\times$  compression ratio but with a significant accuracy drop of 2.1%, even it saves 16.7% end-to-end time over CLICKTRAIN. Figure 15b shows that CLICKTRAIN has 2.1 $\times$  higher compression ratio than PRUNETRAIN with a notable accuracy improvement of 1.1% on ResNet50 with ImageNet but only slightly longer (i.e., 18.4%) end-to-end time. Note that 1.1% on ImageNet and 2.0% on CIFAR10 are significant accuracy improvements considering the limited training time. Thus, aggressively preserving the original architecture is critical for designing PDT-based approaches.

## 7 RELATED WORK

PRUNETRAIN [27] is a state-of-the-art approach to accelerate the DNN training from scratch while pruning it. The work observed that when pruning with group-lasso regularization, once a group of model weights are penalized close to zero, their magnitudes are typically impossible to recover during the rest of the training process. Based on this observation, PRUNETRAIN periodically removes the small weights and reconfigure the network architecture and

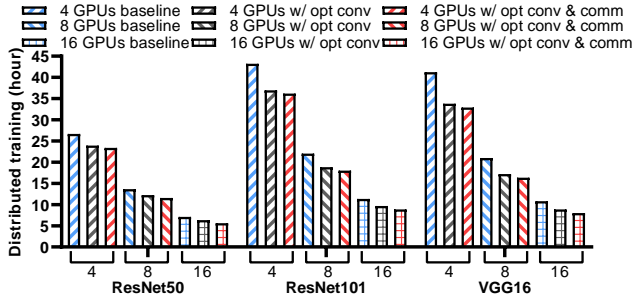


Figure 14: Total time of baseline training and CLICKTRAIN.

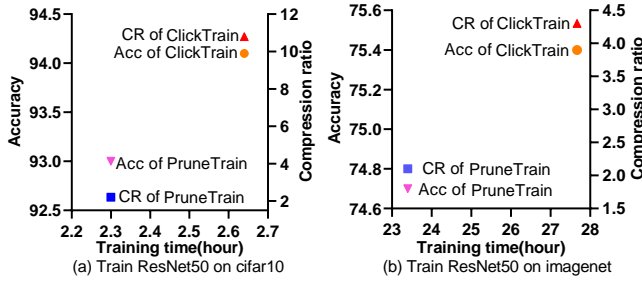


Figure 15: Comparison of PRUNETRAIN and CLICKTRAIN.

hence can gradually reduce the training during training toward both high compression ratio and accuracy. In addition, PRUNETRAIN also proposes to dynamically increase the mini-batch to further increase the training performance. However, as we discussed in Section 3, PRUNETRAIN aggressively change the original network architecture, causing a significant unrecoverable accuracy loss.

The lottery ticket hypothesis [12] proves that subnetworks can match the test accuracy of original network after training for at most the same number of iterations. Those subnetworks are termed as winning tickets, which can be directly trained efficiently. However, it is challenging to determine the architecture of subnetwork.

The Early-Bird (EB) tickets work [49] claims that winning tickets can be identified at a very early training stage using aggressively low-cost training algorithms. Even though EB also adopts the strategy that firstly trains a few epochs and then prunes the network, it chooses channel pruning, which will change the network architecture and lead to a significant accuracy drop.

## 8 CONCLUSION

In this paper, we propose CLICKTRAIN by using dynamic fine-grained pattern-based pruning. It has both algorithm-level and system-level optimizations. Our experimental results on seven DNNs and three datasets demonstrate that PATTERNTRAIN can reduce the cost of the state-of-the-art PAT-based method by up to 2.3× with comparable accuracy and compression ratio. Compared with the state-of-the-art training acceleration approach, PATTERNTRAIN can improve the pruned accuracy by up to 2.0% and the compression ratio by up to 4.9× on the tested CNNs and datasets, with comparable training time. We plan to extend CLICKTRAIN to more types of DNNs in the future.

## ACKNOWLEDGMENTS

This material is based upon work supported by National Science Foundation under Grant No. OAC-2034169, OAC-2042084, CCF-1937500, CNS-1909172, IIS-1850546, IIS-2008973, CNS-1951974. The work was also partially supported by Jeffress Trust Awards in Interdisciplinary Research and Australian Research Council Discovery Project DP210101984. The authors would like to thank TACC for providing access to the Frontera supercomputer.

## REFERENCES

- [1] NVIDIA QUADRO RTX 5000. <https://www.nvidia.com/en-us/design-visualization/quadro/rtx-5000/>, 2020. Online.
- [2] Martin Abadi, Paul Barham, Jianmin Chen, Zhifeng Chen, Andy Davis, Jeffrey Dean, Matthieu Devin, Sanjay Ghemawat, Geoffrey Irving, Michael Isard, Manjunath Kudlur, Josh Levenberg, Rajat Monga, Sherry Moore, Derek Gordon Murray, Benoit Steiner, Paul A. Tucker, Vijay Vasudevan, Pete Warden, Martin Wicke, Yuan Yu, and Xiaoqiang Zheng. Tensorflow: A system for large-scale machine learning. In *12th {USENIX} Symposium on Operating Systems Design and Implementation ({OSDI} 16)*, pages 265–283, 2016.
- [3] Yonathan Aflalo, Asaf Noy, Ming Lin, Itamar Friedman, and Lihi Zelnik. Knapsack pruning with inner distillation. *arXiv preprint arXiv:2002.08258*, 2020.
- [4] Tom B. Brown, Benjamin Mann, Nick Ryder, Melanie Subbiah, Jared Kaplan, Prafulla Dhariwal, Arvind Neelakantan, Pranav Shyam, Girish Sastry, Amanda Askell, Sandhini Agarwal, Ariel Herbert-Voss, Gretchen Krueger, Tom Henighan, Rewon Child, Aditya Ramesh, Daniel M. Ziegler, Jeffrey Wu, Clemens Winter, Christopher Hesse, Mark Chen, Eric Sigler, Mateusz Litwin, Scott Gray, Benjamin Chess, Jack Clark, Christopher Berner, Sam McCandlish, Alec Radford, Ilya Sutskever, and Dario Amodei. Language models are few-shot learners. *arXiv preprint arXiv:2005.14165*, 2020.
- [5] Christopher Choy, JunYoung Gwak, and Silvio Savarese. 4d spatio-temporal convnets: Minkowski convolutional neural networks. In *Proceedings of the IEEE Conference on Computer Vision and Pattern Recognition*, pages 3075–3084, 2019.
- [6] CIFAR-10 and CIFAR-100. <https://www.cs.toronto.edu/~kriz/cifar.html>, 2020. Online.
- [7] Ronan Collobert and Jason Weston. A unified architecture for natural language processing: Deep neural networks with multitask learning. In *Proceedings of the 25th International Conference on Machine Learning*, pages 160–167. ACM, 2008.
- [8] Xiaoliang Dai, Hongxu Yin, and Niraj K Jha. Nest: A neural network synthesis tool based on a grow-and-prune paradigm. *IEEE Transactions on Computers*, 68(10):1487–1497, 2019.
- [9] Peiyan Dong, Siyue Wang, Wei Niu, Chengming Zhang, Sheng Lin, Zhengang Li, Yifan Gong, Bin Ren, Xue Lin, Yanzhi Wang, and Dingwen Tao. Rtmobile: Beyond real-time mobile acceleration of rnns for speech recognition. *arXiv preprint arXiv:2002.11474*, 2020.
- [10] Xuanyi Dong and Yi Yang. Network pruning via transformable architecture search. In *Advances in Neural Information Processing Systems*, pages 759–770, 2019.
- [11] Thomas Elsken, Jan Hendrik Metzen, and Frank Hutter. Neural architecture search: A survey. *arXiv preprint arXiv:1808.05377*, 2018.
- [12] Jonathan Frankle and Michael Carbin. The lottery ticket hypothesis: Finding sparse, trainable neural networks. *arXiv preprint arXiv:1803.03635*, 2018.
- [13] W. T. Freeman and E. H. Adelson. The design and use of steerable filters. *IEEE Transactions on Pattern Analysis and Machine Intelligence*, 13(9):891–906, 1991.
- [14] Trevor Gale, Matei Zaharia, Cliff Young, and Erich Elsen. Sparse gpu kernels for deep learning. *arXiv preprint arXiv:2006.10901*, 2020.
- [15] Song Han, Xingyu Liu, Huizi Mao, Jing Pu, Ardavan Pedram, Mark Horowitz, and Bill Dally. Deep compression and eie: Efficient inference engine on compressed deep neural network. In *Hot Chips Symposium*, pages 1–6, 2016.
- [16] Kaiming He, Xiangyu Zhang, Shaoqing Ren, and Jian Sun. Deep residual learning for image recognition. In *Proceedings of the IEEE conference on computer vision and pattern recognition*, pages 770–778, 2016.
- [17] Yang He, Guoliang Kang, Xuanyi Dong, Yanwei Fu, and Yi Yang. Soft filter pruning for accelerating deep convolutional neural networks. In *Proceedings of the 27th International Joint Conference on Artificial Intelligence*, pages 2234–2240, 2018.
- [18] Yihui He, Xiangyu Zhang, and Jian Sun. Channel pruning for accelerating very deep neural networks. In *Proceedings of the IEEE International Conference on Computer Vision*, pages 1398–1406. IEEE, 2017.
- [19] Guyue Huang, Guohao Dai, Yu Wang, and Huazhong Yang. Ge-spm: General-purpose sparse matrix-matrix multiplication on gpus for graph neural networks. *arXiv preprint arXiv:2007.03179*, 2020.
- [20] Sian Jin, Sheng Di, Xin Liang, Jiannan Tian, Dingwen Tao, and Franck Cappello. Deepisz: A novel framework to compress deep neural networks by using error-bounded lossy compression. In *Proceedings of the 28th International Symposium*

- on High-Performance Parallel and Distributed Computing, pages 159–170. ACM, 2019.
- [21] Alex Krizhevsky, Ilya Sutskever, and Geoffrey E Hinton. Imagenet classification with deep convolutional neural networks. In *Advances in neural information processing systems*, pages 1097–1105, 2012.
  - [22] Large Scale Visual Recognition Challenge. <http://www.image-net.org/challenges/LSVRC/>, 2020. Online.
  - [23] Shaohui Lin, Rongrong Ji, Chenqian Yan, Baochang Zhang, Liujuan Cao, Qixiang Ye, Feiyue Huang, and David Doermann. Towards optimal structured cnn pruning via generative adversarial learning. In *Proceedings of the IEEE Conference on Computer Vision and Pattern Recognition*, pages 2790–2799, 2019.
  - [24] Zhuang Liu, Mingjie Sun, Tinghui Zhou, Gao Huang, and Trevor Darrell. Re-thinking the value of network pruning. *arXiv preprint arXiv:1810.05270*, 2018.
  - [25] Justin Luitjens. CUDA Pro Tip: Increase Performance with Vectorized Memory Access. <https://developer.nvidia.com/blog/cuda-pro-tip-increase-performance-with-vectorized-memory-access/>, 2013. Online.
  - [26] Jian-Hao Luo, Jianxin Wu, and Weiyao Lin. Thinet: A filter level pruning method for deep neural network compression. In *Proceedings of the IEEE international conference on computer vision*, pages 5058–5066, 2017.
  - [27] Sangkug Lym, Esha Choukse, Siavash Zangeneh, Wei Wen, Sujay Sanghavi, and Mattan Erez. Prunetrain: fast neural network training by dynamic sparse model reconfiguration. In *Proceedings of the International Conference for High Performance Computing, Networking, Storage and Analysis*, pages 1–13, 2019.
  - [28] Xiaolong Ma, Fu-Ming Guo, Wei Niu, Xue Lin, Jian Tang, Kaisheng Ma, Bin Ren, and Yanzhi Wang. Pconv: The missing but desirable sparsity in dnn weight pruning for real-time execution on mobile devices. *arXiv preprint arXiv:1909.05073*, 2019.
  - [29] Xiaolong Ma, Zhengang Li, Yifan Gong, Tianyun Zhang, Wei Niu, Zheng Zhan, Pu Zhao, Jian Tang, Xue Lin, Bin Ren, and Yanzhi Wang. Blk-rew: A unified block-based dnn pruning framework using reweighted regularization method. *arXiv preprint arXiv:2001.08357*, 2020.
  - [30] Xiaolong Ma, Sheng Lin, Shaokai Ye, Zhezhi He, Linfeng Zhang, Geng Yuan, Sia Huat Tan, Zhengang Li, Deliang Fan, Xuehai Qian, Xue Lin, Kaisheng Ma, and Yanzhi Wang. Non-structured dnn weight pruning – is it beneficial in any platform?, 2019.
  - [31] Xiaolong Ma, Wei Niu, Tianyun Zhang, Sijia Liu, Fu-Ming Guo, Sheng Lin, Hongjia Li, Xiang Chen, Jian Tang, Kaisheng Ma, Bin Ren, and Yanzhi Wang. An image enhancing pattern-based sparsity for real-time inference on mobile devices. *arXiv preprint arXiv:2001.07710*, 2020.
  - [32] Lukas Meier, Sara Van De Geer, and Peter Bühlmann. The group lasso for logistic regression. *Journal of the Royal Statistical Society: Series B (Statistical Methodology)*, 70(1):53–71, 2008.
  - [33] Pavlo Molchanov, Arun Mallya, Stephen Tyree, Iuri Frosio, and Jan Kautz. Importance estimation for neural network pruning. In *Proceedings of the IEEE Conference on Computer Vision and Pattern Recognition*, pages 11264–11272, 2019.
  - [34] Pavlo Molchanov, Stephen Tyree, Tero Karras, Timo Aila, and Jan Kautz. Pruning convolutional neural networks for resource efficient inference. *arXiv preprint arXiv:1611.06440*, 2016.
  - [35] M Naumov, LS Chien, P Vandermersch, and U Kapasi. Cuspars library. In *GPU Technology Conference*, 2010.
  - [36] Wei Niu, Xiaolong Ma, Sheng Lin, Shihao Wang, Xuehai Qian, Xue Lin, Yanzhi Wang, and Bin Ren. Patdnn: Achieving real-time dnn execution on mobile devices with pattern-based weight pruning. In *Proceedings of the Twenty-Fifth International Conference on Architectural Support for Programming Languages and Operating Systems (ASPLOS)*, 2020.
  - [37] intel Xeon E5-2680 v4 vs Qualcomm SM8150 Snapdragon 855. <https://gadgetversus.com/processor/intel-xeon-e5-2680-v4-vs-qualcomm-sm8150-snapdragon-855/>, 2020. Online.
  - [38] CUDA Nvidia. Cublas library. *NVIDIA Corporation, Santa Clara, California*, 15(27):31, 2008.
  - [39] Adam Paszke, Sam Gross, Francisco Massa, Adam Lerer, James Bradbury, Gregory Chanan, Trevor Killeen, Zeming Lin, Natalia Gimelshein, Luca Antiga, Alban Desmaison, Andreas Köpf, Edward Yang, Zachary DeVito, Martin Raison, Alykhan Tejani, Sasank Chilamkurthy, Benoit Steiner, Lu Fang, Junjie Bai, and Soumith Chintala. Pytorch: An imperative style, high-performance deep learning library. In *Advances in Neural Information Processing Systems*, pages 8024–8035, 2019.
  - [40] Masuma Akter Rumi, Xiaolong Ma, Yanzhi Wang, and Peng Jiang. Accelerating sparse cnn inference on gpus with performance-aware weight pruning. In *Proceedings of the ACM International Conference on Parallel Architectures and Compilation Techniques*, pages 267–278, 2020.
  - [41] Karen Simonyan and Andrew Zisserman. Very deep convolutional networks for large-scale image recognition. *arXiv preprint arXiv:1409.1556*, 2014.
  - [42] Dan Stanzione, John West, R Todd Evans, Tommy Minyard, Omar Ghattas, and Dhabaleswar K Panda. Frontera: The evolution of leadership computing at the national science foundation. In *Practice and Experience in Advanced Research Computing*, pages 106–111, 2020.
  - [43] Christian Szegedy, Wei Liu, Yangqing Jia, Pierre Sermanet, Scott Reed, Dragomir Anguelov, Dumitru Erhan, Vincent Vanhoucke, and Andrew Rabinovich. Going deeper with convolutions. In *Proceedings of the IEEE conference on Computer Vision and Pattern Recognition*, pages 1–9, 2015.
  - [44] Hao Wang, Naiyan Wang, and Dit-Yan Yeung. Collaborative deep learning for recommender systems. In *Proceedings of the 21th ACM SIGKDD international conference on knowledge discovery and data mining*, pages 1235–1244. ACM, 2015.
  - [45] Linnan Wang, Jinmian Ye, Yiyang Zhao, Wei Wu, Ang Li, Shuaiwen Leon Song, Zenglin Xu, and Tim Kraska. Superneurons: dynamic gpu memory management for training deep neural networks. In *Proceedings of the 23rd ACM SIGPLAN Symposium on Principles and Practice of Parallel Programming*, pages 41–53, 2018.
  - [46] Yulong Wang, Xiaolu Zhang, Lingxi Xie, Jun Zhou, Hang Su, Bo Zhang, and Xiaolin Hu. Pruning from scratch. In *Proceedings of the AAAI Conference on Artificial Intelligence*, volume 34, pages 12273–12280, 2020.
  - [47] Tien-Ju Yang, Yu-Hsin Chen, and Vivienne Sze. Designing energy-efficient convolutional neural networks using energy-aware pruning. In *Proceedings of the IEEE Conference on Computer Vision and Pattern Recognition*, pages 5687–5695, 2017.
  - [48] Zhuliang Yao, Shijie Cao, Wencong Xiao, Chen Zhang, and Lanshun Nie. Balanced sparsity for efficient dnn inference on gpu. In *Proceedings of the AAAI Conference on Artificial Intelligence*, volume 33, pages 5676–5683, 2019.
  - [49] Haoran You, Chaojian Li, Pengfei Xu, Yonggan Fu, Yue Wang, Xiaohan Chen, Richard G Baraniuk, Zhangyang Wang, and Yingyan Lin. Drawing early-bird tickets: Towards more efficient training of deep networks. *arXiv preprint arXiv:1909.11957*, 2019.
  - [50] Zhonghui You, Kun Yan, Jinmian Ye, Meng Ma, and Ping Wang. Gate decorator: Global filter pruning method for accelerating deep convolutional neural networks. In *Advances in Neural Information Processing Systems*, pages 2133–2144, 2019.
  - [51] Ruichi Yu, Ang Li, Chun-Fu Chen, Jui-Hsin Lai, Vlad I Morariu, Xintong Han, Mingfei Gao, Ching-Yung Lin, and Larry S Davis. Nisp: Pruning networks using neuron importance score propagation. In *Proceedings of the IEEE Conference on Computer Vision and Pattern Recognition*, pages 9194–9203, 2018.
  - [52] Geng Yuan, Xiaolong Ma, Caiwen Ding, Sheng Lin, Tianyun Zhang, Zeinab S Jalali, Yilong Zhao, Li Jiang, Sucheta Soundarajan, and Yanzhi Wang. An ultra-efficient memristor-based dnn framework with structured weight pruning and quantization using admm. In *2019 IEEE/ACM International Symposium on Low Power Electronics and Design (ISLPED)*, pages 1–6. IEEE, 2019.
  - [53] Tianyun Zhang, Shaokai Ye, Kaiqi Zhang, Jian Tang, Wujie Wen, Makan Fardad, and Yanzhi Wang. A systematic dnn weight pruning framework using alternating direction method of multipliers. In *Proceedings of the European Conference on Computer Vision (ECCV)*, pages 184–199, 2018.
  - [54] Zhuangwei Zhuang, Minghui Tan, Bohan Zhuang, Jing Liu, Yong Guo, Qingyao Wu, Junzhou Huang, and Jinhui Zhu. Discrimination-aware channel pruning for deep neural networks. In *Advances in Neural Information Processing Systems*, pages 875–886, 2018.